Inorganic Chemistry

ARTICLE

pubs.acs.org/IC

Metallacyclophanes of 1,6-Bis(diphenylphosphino)pyrene: Excimeric Emission and Effect of Oxygen on Stability of the Rings

Jian Hu, Minh-Hai Nguyen, and John H. K. Yip*

Department of Chemistry, National University of Singapore, 3 Science Drive 3, Singapore 117543, Singapore

Supporting Information

ABSTRACT: 1,6-Bis(diphenylphosphino)pyrene (L) was reacted with Ag(I) and Cu(I) ions to form metallacyclophanes $[Ag_2L_2(OTf)_2]$ (**1**), $[Cu_2L_2(MeCN)_4]^{2+}$ (**2**), and $[Cu_2L_2I_2]$ (**3**) which consisted of two cofacial pyrenyl rings. **1** and **2** exhibited intramolecular excimeric emissions which along with the UV−vis absorption were invoked in understanding the solution dynamics of the metallocyclophanes. The metallacyclophanes were stable toward ring-opening dissociation at concentration as low as 10^{-7} M. However, air oxidation of the dangling PPh_2 groups arising from metal−ligand bond dissociation drove the equilibrium toward dissociation and produced the oxidized phosphine 1,6-bis(diphenylphosphine oxide)pyrene.

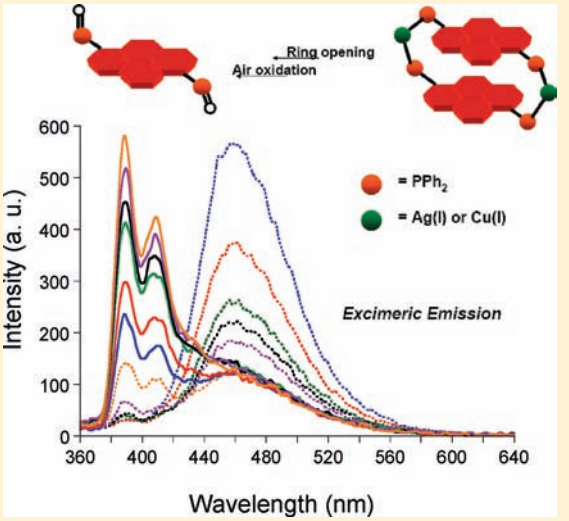

INTRODUCTION

The rich photophysics of polycyclic aromatic hydrocarbons is well illustrated by pyrene which apart from $S_1 \rightarrow S_0$ fluorescence displays P-type delayed fluorescence[1] and excimeric emission.[1,2] In addition, heavy atoms can switch on $T_1 \rightarrow S_0$ phosphorescence.[3] For example, it was recently demonstrated that attaching Au(I)[4a,b] and Pt(II)[4b,c] ions to pyrene can enhance $T_1 \rightarrow S_0$ phosphorescence with emission quantum yield up to 1.5×10^{-2}.[4c] At high concentration, a molecule in the S_1 excited state can form an excimer complex with another molecule in the S_0 ground state. Emission of the excimer, which is lower in energy than the fluorescence of the monomer and unstructured, has been harnessed for chemical sensing.[5] Orientation of the pyrene rings is crucial to the formation of the excimer and its emission energy. Calculations have suggested eclipsed conformation is the equilibrium geometry for the excimer,[2,6] and staggered conformations generally lead to blue-shifts of the excimeric emission.

Although the excimeric emission of pyrene has been widely used for luminescent sensing, there is little information on the conformational structures of the excimers involved,[7] though a few structures have been proposed by molecular modeling.[8] Recently we reported phosphorescent cyclometalated Pt(II) complexes of 1,6-bis(diphenylphosphino)pyrene (L, Scheme 1) and 1-diphenylphosphinopyrene (L′, Scheme 1) in which the ligands form chelate rings with the metal ions.[4c]

In the present study, we demonstrate that L can form metallacyclophanes $[Ag_2L_2(OTf)_2]_n$ (**1**), $[Cu_2L_2(MeCN)_4](PF_6)_2$ (**2**·$(PF_6)_2$), and $[Cu_2L_2I_2]$ (**3**) which consist of two cofacial pyrene rings (Scheme 1).

The complexes **1** and **2** exhibit intramolecular excimeric emissions and can be regarded as models for excimers of different conformations. Luminescent metallacyclophanes[9] have attracted a lot of recent attention mainly because of their structures and guest binding. On the other hand, solution dynamics and stability of metallacyclophanes have not been widely pursued,[10] mostly because of the lack of a suitable spectroscopic handle in many systems by which the dynamics can be followed. The excimeric emissions and intense ligand-centered absorptions of **1**−**3** allow their solution dynamics to be traced. Our results show that air oxidation of L influences the solution dynamics of the metallacyclophanes. The compounds $[AgL'_2](OTf)$ (**4**), $[Au_2Cl_2L]$ (**5**), and 1,6-bis(diphenylphosphine oxide)pyrene (**6**) were synthesized as monomer analogue of the metallacyclophanes and reference for ligand oxidation.

EXPERIMENTAL SECTION

General Methods. All syntheses were carried out in a dry N_2 atmosphere using standard Schlenk technique unless otherwise stated. All reagents and solvents used for syntheses were used as received. Solvents used for spectroscopic measurements were purified according

Received: December 7, 2010
Published: July 19, 2011

Scheme 1

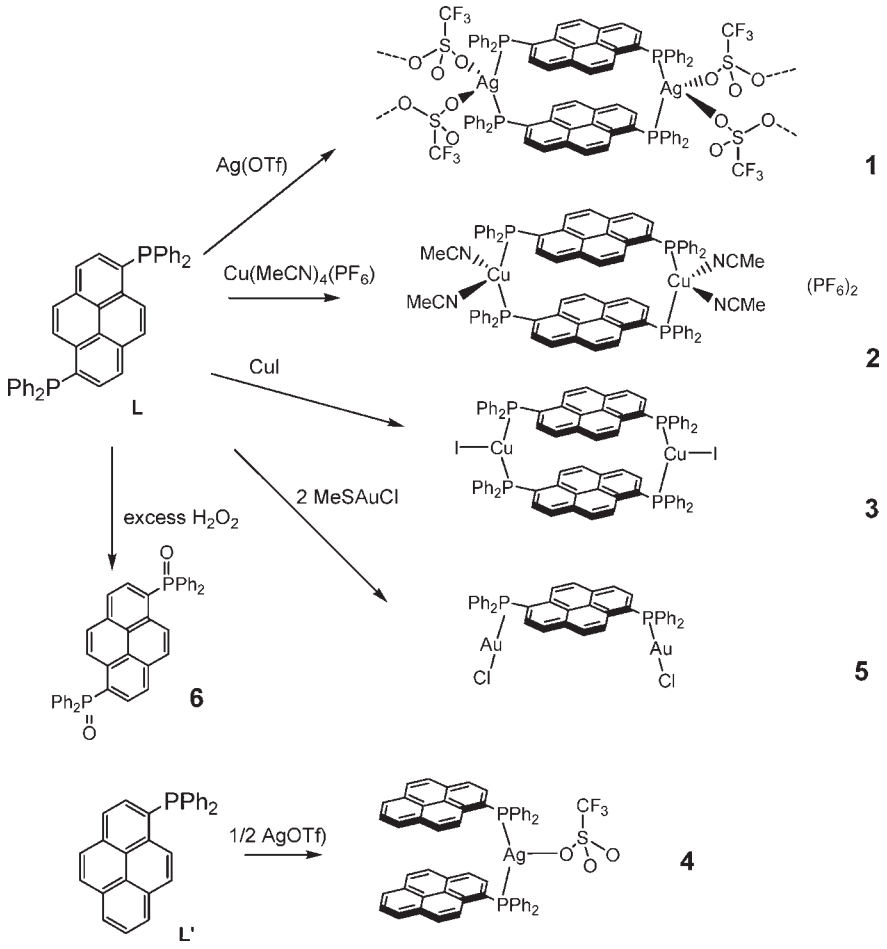

to the literature procedures. $[Cu(MeCN)_4](PF_6)$[11] and CuI[12] were prepared according to published methods. L and L′ were prepared according to reported methods.[4c]

Physical Measurements. The UV−vis absorption and room temperature emission spectra of the complexes were recorded on a Shimadzu UV-1601 UV−visible spectrophotometer and a Perkin-Elmer LS-50B luminescence spectrometer, respectively. The emission quantum yields were measured with anthracene as standard. NMR experiments were performed on a Bruker ACF 300, AMX500 or DRX500 spectrometer. Electrospray ionization mass spectra (ESI-MS) were measured on a Finnigan MAT 731 LCQ spectrometer. Fast atom bombardment mass spectra (FAB-MS) were measured on a Finnigan MAT 95 XL-S spectrometer (Cs gun, matrix: 3-nitrobenzyl alcohol). Elemental analyses of the complexes were carried out at the Elemental Analysis Laboratory in the National University of Singapore.

Synthesis of $[Ag_2L_2(OTf)_2]$ (1). L (208 mg, 0.365 mmol) and AgOTf (94 mg, 0.366 mmol) were mixed in MeCN (25 mL), and the mixture was stirred for 4 h. The resulting solution was concentrated, and excess Et_2O was added to precipitate the pale yellow product. Single crystals suitable for X-ray diffraction were obtained from CH_2Cl_2/Et_2O by slow diffusion. Yield: 0.28 g, 93%. Anal. Calcd (%) for $[C_{82}H_{56}Ag_2F_6O_6P_4S_2]_n$: C, 59.51; H, 3.41. Found (%): C, 59.06; H, 3.40. ^{1}H NMR (CD_2Cl_2, 300 MHz): δ/ppm 8.08 (d, J = 9 Hz, 2H, $H_{5,10}$ of pyrene ring), 7.72−7.66 (m, 10H, H_{Ph}), 7.58 (d, J = 8 Hz, 2H, $H_{3,8}$ of pyrene ring), 7.45−7.41 (m, 6H, H_{Ph}), 7.34−7.28 (m, 6H, $H_{2,7}$ of pyrene ring and H_{Ph}), 6.99 (d, J = 9 Hz, 2H, $H_{4,9}$ of pyrene ring). $^{31}P\{^1H\}$ NMR (CD_2Cl_2, 121.5 MHz): δ/ppm 3.98 (d); $^1J(^{107}Ag-P)$ = 478 Hz, $^1J(^{109}Ag-P)$ = 551 Hz. FAB-Mass (m/z): 1505.4 $[Ag_2L_2(OTf)]^+$, 1249.4 $[Ag_2L_2]^+$, 677.1 $[AgL]^+$.

Synthesis of $[Cu_2L_2(MeCN)_4](PF_6)_2$ ($2\cdot(PF_6)_2$). L (210 mg, 0.368 mmol) and $[Cu(CH_3CN)_4](PF_6)$ (137 mg, 0.368 mmol) were added into 50 mL of CH_2Cl_2. The mixture was stirred for 3 h and then filtered. The filtrate was concentrated under reduced pressure, and Et_2O was added to precipitate the pale yellow product. Crystals suitable for X-ray diffraction were obtained from $CH_2Cl_2/CH_3CN/Et_2O$ by slow diffusion. Yield: 0.24 g, 70%. Anal. Calcd (%) for $C_{88}H_{68}Cu_2F_{12}N_4P_6$: C, 61.36; H, 3.98. Found (%): C, 61.14; H, 3.92. ^{1}H NMR (CD_2Cl_2, 300 MHz): δ/ppm 7.87 (d, J = 9 Hz, 2H, $H_{5,10}$ of pyrene ring), 7.75−7.72 (m, 2H, H_{Ph}), 7.69−7.64 (m, 10H, $H_{3,8}$ of pyrene ring and H_{Ph}), 7.50−7.47 (m, 2H, H_{Ph}), 7.40−7.37 (m, 6H, $H_{2,7}$ of pyrene ring and H_{Ph}), 7.35−7.32 (m, 4H, H_{Ph}), 7.00 (d, J = 9 Hz, 2H, $H_{4,9}$ of pyrene ring), 2.11 (s, 6H, CH_3CN). $^{31}P\{^1H\}$ NMR (CD_2Cl_2, 121.5 MHz): δ/ppm −4.14 (s, P of L), −143.81 (heptet, PF_6, ^1J(P−F) = 711 Hz). FAB-Mass (m/z): 1413.3 $[Cu_2L_2(PF_6)]^+$, 1285.3 $[CuL_2(MeCN)_2]^+$, 1203.4 $[CuL_2]^+$.

Synthesis of $[Cu_2L_2I_2]$ (3). L (424 mg, 0.743 mmol) and CuI (141 mg, 0.740 mmol) were added into 50 mL of CH_2Cl_2 under N_2. The mixture was stirred for 3 h and then filtered. The filtrate was concentrated by rotaevaporation and Et_2O was added to obtain the yellow solid. Single crystals suitable for X-ray diffraction were obtained from CH_2Br_2/Et_2O by slow diffusion. Yield: 0.52 g, 90%. Anal. Calcd (%) for $C_{80}H_{56}Cu_2I_2P_4$: C, 63.13; H, 3.71. Found (%): C, 63.39; H, 3.59. ^{1}H NMR ($CDCl_3$, 300 MHz): 8.02 (d, J = 9 Hz, 2H, $H_{5,10}$ of pyrene ring), 7.71 (unresolved multiplet, 8H, H_{Ph}), 7.59−7.58 (m, 6H, H_{Ph}),

dx.doi.org/10.1021/ic102441b |*Inorg. Chem.* 2011, 50, 7429–7439

Table 1. X-ray Data for $1\cdot 4Et_2O$, $2\cdot(PF_6)_2\cdot MeCN\cdot Et_2O\cdot 0.5H_2O$, $3\cdot CH_2Br_2\cdot Et_2O$, 4, 5, and 6

	$1\cdot 4(Et_2O)$	$2\cdot(PF_6)_2\cdot(MeCN)\cdot(Et_2O)$ $1/2(H_2O)$	$3\cdot(CH_2Br_2)(Et_2O)$	4	5	6
empirical formula	$C_{98}H_{96}Ag_2F_6O_{10}P_4S_2$	$C_{94}H_{81}Cu_2F_{12}N_5O_{1.5}P_6$	$C_{85}H_{68}Br_2Cu_2I_2OP_4$	$C_{57}H_{38}AgF_3O_3P_2S$	$C_{40}H_{28}Au_2Cl_2P_2$	$C_{40}H_{28}O_2P_2$
formula weight ($g\ mol^{-1}$)	1951.49	1845.54	1769.97	1029.74	1035.4	602.56
temperature (K)	223(2)	213(2)	293(2)	223(2)	223(2)	223(2)
crystal system	monoclinic	monoclinic	monoclinic	monoclinic	orthorhombic	triclinic
space group	$C2/c$	$P2_1/c$	$P2_1/c$	$P2_1/c$	$P2_12_12_1$	$P\bar{1}$
unit cell dimensions						
a, Å	33.243(7)	19.8148(9)	12.485(4)	11.3616(4)	12.3088(8)	9.1022(5)
b, Å	13.339(3)	20.6818(8)	16.178(5)	19.8387(8)	15.1451(10)	9.5051(5)
c, Å	24.388(6)	22.1823(10)	39.625(12)	20.8318(8)	20.5140(14)	9.9259(6)
α, deg	90	90	90	90	90	67.706(1)
β, deg	116.413(8)	106.899(1)	96.866(5)	103.567(1)	90	71.735(1)
γ, deg	90	90	90	90	90	77.666(1)
volume ($Å^3$)	9686(4)	8697.9(7)	7946(4)	4564.5(3)	3824.2(4)	750.14(7)
Z	4	4	4	4	4	1
density (calcd/$g\ cm^{-3}$)	1.338	1.409	1.479	1.498	1.798	1.334
absorption coefficient (mm^{-1})	0.580	0.677	2.442	0.617	7.913	0.182
$F(000)$	4016	3792	3520	2096	1960	314
crystal size (mm^3)	0.36 × 0.28 × 0.20	0.50 × 0.14 × 0.10	0.36 × 0.24 × 0.10	0.36 × 0.24 × 0.20	0.10 × 0.12 × 0.20	0.60 × 0.32 × 0.26
θ range for data collection	1.67 to 25.00°	1.37 to 25.00°	1.63 to 24.00°	1.84 to 27.50°	1.93 to 25.00°	2.29 to 27.50°
index ranges	$-39 \le h \le 9$	$-19 \le h \le 23$	$-9 \le h \le 4$	$-14 \le h \le 10$	$-14 \le h \le 4$	$-11 \le h \le 11$
	$-15 \le k \le 15$	$-20 \le k \le 24$	$-18 \le k \le 8$	$-25 \le k \le 25$	$-11 \le k \le 8$	$-12 \le k \le 12$
	$-29 \le l \le 29$	$-26 \le l \le 24$	$-45 \le l \le 45$	$-26 \le l \le 27$	$-24 \le l \le 24$	$-12 \le l \le 12$
reflections collected	51114	50486	37082	32432	21980	9892
iIndependent reflections	8523 [R(int) = 0.0495]	15324 [R(int) = 0.1228]	12474 [R(int) = 0.1359]	10477 [R(int) = 0.0468]	6715 [R(int) = 0.0596]	3427 [R(int) = 0.0211]
goodness-of-fit on F^{2a}	1.037	1.012	1.147	1.062	1.150	1.051
final R indices $[I > 2\sigma(I)]^b$	$R1$ = 0.0858	$R1$ = 0.0868	$R1$ = 0.1490	$R1$ = 0.0697	$R1$ = 0.0593	$R1$ = 0.0479
	$wR2$ = 0.2292	$wR2$ = 0.1828	$wR2$ = 0.3614	$wR2$ = 0.1703	$wR2$ = 0.1498	$wR2$ = 0.1267
R indices (all data)	$R1$ = 0.1015	$R1$ = 0.1723	$R1$ = 0.2101	$R1$ = 0.0923	$R1$ = 0.0666	$R1$ = 0.0518
	$wR2$ = 0.2429	$wR2$ = 0.2194	$wR2$ = 0.3891	$wR2$ = 0.1837	$wR2$ = 0.1527	$wR2$ = 0.1298
largest diff. peak and hole ($e\ Å^{-3}$)	3.756, −0.706	1.018, −0.435	3.099, −1.075	4.516, −0.350	3.067, −2.779	0.529, −0.215

For all crystal determinations, scan type and wavelength of radiation used is ω and 0.71073 Å, respectively [a] GOF = $[(w(F_o^2 - F_c^2)^2/(n-p)]^{1/2}$. [b] R1 = $(||F_o| - |F_c||)/(|F_o|)$; wR2 = $[w(F_o^2 - F_c^2)/w(F_o^4)]^{1/2}$

7.50 (d, J = 8 Hz, 2H, $H_{3,8}$ of pyrene ring), 7.38−7.35 (m, 2H, H_{Ph}), 7.27−7.26 (m, 6H, $H_{2,7}$ of pyrene ring and H_{Ph}), 6.86 (d, J = 9 Hz, 2H, $H_{4,9}$ of pyrene ring). $^{31}P\{^1H\}$ NMR ($CDCl_3$, 121.5 MHz): −7.66 (s). ESI-Mass (m/z): 1394.9 (100%) $[Cu_2L_2I]^+$, 634.4 (15%) $[Cu_2L_2]^{2+}$ (Supporting Information, Figure S1). FAB-Mass (m/z): 1395.2 $[Cu_2L_2I]^+$, 1203.4 $[CuL_2]^+$, 633.1 $[CuL]^+$.

Synthesis of $[AgL'_2(OTf)]$ (4). L′ (285 mg, 0.738 mmol) and AgOTf (95 mg, 0.370 mmol) were added into 25 mL of CH_3CN, and the mixture was stirred for 2 days in dark. All solvent was removed by rotaevaporation. The product was redissolved in CH_2Cl_2, followed by addition of isooctane to give the pale yellow powder. Single crystals were obtained from CH_2Cl_2/Et_2O by slow diffusion. Yield: 285 mg, 75%. Anal. Calcd (%) for $C_{57}H_{38}AgF_3O_3P_2S$: C, 66.48; H, 3.72. Found (%): C, 66.21; H, 3.61. ^1H NMR ($CDCl_3$, 300 MHz): δ/ppm 8.23 (d, $^3J_{H-H}$ = 9 Hz, 1H, H_{10} of pyrene ring), 8.14 (d, J = 7 Hz, 1H), 7.99 (d, J = 9 Hz, 1H, H_9 of pyrene ring), 7.94−7.89 (m, 1H), 7.78−7.69 (m, 3H), 7.41−7.17 (m, 12H). $^{31}P\{^1H\}$ NMR ($CDCl_3$, 121.5 MHz): δ/ppm 4.01 (d, not well resolved); $^1J(Ag^{107}\text{-}P)$ = 487 Hz, $^1J(Ag^{109}\text{-}P)$ = 539 Hz. ESI-Mass (m/z): 881.2(25%) $[AgL'_2]^+$.

Synthesis of $[Au_2Cl_2L]$ (5). L (859 mg, 1.505 mmol) and $Au(SMe_2)Cl$ (983 mg, 3.012 mmol) were dissolved in 150 mL of CH_2Cl_2 under N_2, the mixture was stirred for 1.5 h in dark, followed by filtration. The filtrate was concentrated by rotaevaporation and Et_2O was added to precipitate the pale yellow product. Single crystals suitable for X-ray diffraction were obtained from CH_2Cl_2/Et_2O by slow diffusion. Yield: 1.00 g, 64%. Anal. Calcd (%) for $C_{40}H_{28}Au_2Cl_2P_2$: C, 46.40; H, 2.73. Found (%): C, 46.37; H, 2.61. ^1H NMR ($CDCl_3$, 300 MHz): δ/ppm 8.88 (dd, $^3J_{H-H}$= 9 Hz, $^3J_{H-P}$ = 1 Hz, 2H, $H_{5,10}$ of pyrene ring), 8.15 (dd, $^3J_{H-H}$ = 9 Hz, $^4J_{H-P}$ = 1 Hz, 2H, $H_{2,7}$ of pyrene ring), 8.10 (d, J = 9 Hz, 2H, $H_{4,9}$ of pyrene ring), 7.68−7.47 (m, 22H, unresolved).

dx.doi.org/10.1021/ic102441b |Inorg. Chem. 2011, 50, 7429–7439

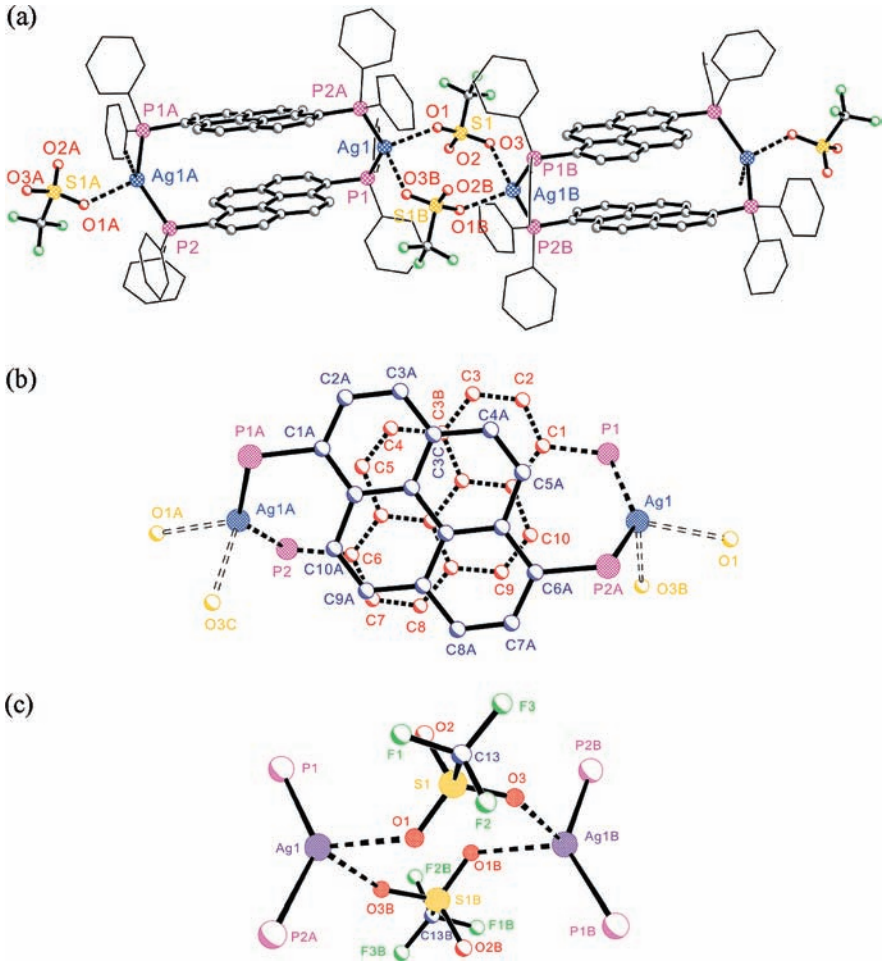

Figure 1. (a) ORTEP diagram of $\mathbf{1}\cdot 4Et_2O$ with 50% thermal ellipsoids. H atoms and solvent molecules are omitted, and phenyl rings are shown in wire-frame style for clarity. (b) top view showing the orientation of the pyrene rings, (c) puckered chairlike conformation of the 8-membered ring composed of Ag and OTf ions.

$^{31}P\{^1H\}$ NMR ($CDCl_3$, 121.5 MHz): δ/ppm 27.10 (s). ESI-Mass (m/z): 1001.1 (100%) $[Au_2LCl]^+$.

Synthesis of 1,6-Bis(diphenylphosphine oxide)pyrene (6). Excess 30 wt % H_2O_2 solution (10 mL) was added into a suspension of L (0.50 g, 0.876 mmol) in MeOH (100 mL). The mixture was stirred for 24 h. Water (100 mL) was added into the suspension, and the product was then extracted by CH_2Cl_2 and purified by column chromatography on silica gel with ethyl acetate as the eluent. Single crystals suitable for X-ray diffraction were obtained from CH_2Cl_2/Hexane. Yield: 0.45 g, 85%. Anal. Calcd (%) for $C_{40}H_{28}O_2P_2$: C, 79.73; H, 4.68. Found (%): C, 79.83; H, 4.59. ^1H NMR ($CDCl_3$, 300 MHz): δ/ppm 9.12 (d, $^3J_{H-H}$ = 9 Hz, 2H, $H_{5,10}$ of pyrene ring), 8.10 (dd, $^3J_{H-H}$ = 8 Hz, $^3J_{H-P}$ = 2.3 Hz, 2H, $H_{2,7}$ of pyrene ring), 8.06 (d, $^3J_{H-H}$ = 9 Hz, 2H, $H_{4,9}$ of pyrene ring), 7.88 (d, $^3J_{H-H}$ = 8 Hz, 2H, $H_{3,8}$ of pyrene ring), 7.76−7.68 (m, 8H, H_{Ph}), 7.58−7.7.45 (m, 12H, H_{Ph}). $^{31}P\{^1H\}$ NMR ($CDCl_3$, 121.5 MHz): δ/ppm 33.42 (s).

X-ray Crystallography. The diffraction experiments were carried out on a Bruker AXS SMART CCD 3-circle diffractometer with a sealed tube at 223 K using graphite-monochromated Mo Kα radiation (λ = 0.71073 Å). The software used were as follows: SMART[13a] for collecting frames of data, indexing reflection, and determination of lattice parameters; SAINT[13a] for integration of intensity of reflections and scaling; SADABS[13b] for empirical absorption correction; and SHELXTL[13c] for space group determination, structure solution, and least-squares refinements on $|F|$.[2] Anisotropic thermal parameters were refined for the rest of the non-hydrogen atoms. The hydrogen atoms were placed in their ideal positions. The crystal data and details of data collection and refinement are summarized in Table 1.

RESULTS AND DISCUSSION

Synthesis. Reaction of the bidentate phosphine L with AgOTf, $CuPF_6$, or CuI in 1:1 ratio gave binuclear metallacyclophanes **1**, $\mathbf{2}\cdot(PF_6)_2$, and **3** as the major products (Scheme 1). The high yields (70−90%) of the metallacyclophanes and the fact that similar macrocyclic structures were formed with different metal ions (Ag^+ and Cu^+) and different ligands (iodide and acetonitrile in **2** and **3**) suggests the metallacyclophanes are thermodynamically favored. Single crystals were obtained from diffusion of diethyl ether into CH_2Cl_2 or CH_2Br_2 solutions of the complexes. The complexes were characterized by elemental analysis, ESI-MS or FAB-MS, ^1H and $^{31}P\{^1H\}$ NMR, and single crystal X-ray diffraction. FAB-MS spectra of the metallacyclophanes show peaks which correspond to $[Ag_2L_2(OTf)]^+$ (m/z 1505.4), $[Cu_2L_2(PF_6)]^+$ (m/z 1413.3), and $[Cu_2L_2I]^+$ (m/z 1395.2). It indicates that the complexes retain their macrocyclic structures in solutions. Complex **4** was synthesized from reaction of L′ and 0.5 mol. equiv. of AgOTf. A binuclear gold(I) complex of L (**5**) was prepared by reacting L with 2 mol. equiv. of

dx.doi.org/10.1021/ic102441b |Inorg. Chem. 2011, 50, 7429–7439

Table 2. Selected Bond Lengths and Angles for $1 \cdot 4Et_2O$

bond lengths (Å)		bond angles (deg)	
Ag(1)−P(1)	2.4668(18)	O(1)−Ag(1)−P(1)	121.58(14)
Ag(1)−P(2A)	2.4753(19)	O(1)−Ag(1)−P(2A)	96.64(13)
Ag(1)−O(1)	2.437(5)	O(1)−Ag(1)−O(3B)	84.29(11)
Ag(1)−O(3B)	2.608(6)	P(1)−Ag(1)−P(2A)	136.71(6)
		P(1)−Ag(1)−O(3B)	96.62(6)
		P(2A)−Ag(1)−O(3B)	107.50(11)

Me_2SAuCl. Oxidation of L by excess H_2O_2 gave 1,6-bis-(diphenylphosphine oxide)pyrene (**6**). Both **5** and **6** served as references in the study of the spectroscopy and solution dynamics of the metallacyclophanes.

Structures. Figure 1 shows the X-ray crystal structure of $1 \cdot 4Et_2O$ (Table 2 for selected bond lengths and angles). The complex displays a macrocyclic structure composed of two ligands L connected by two Ag ions which are related by 2-fold rotation. Each Ag ion is coordinated to two P atoms from L and two O atoms from two OTf ions, showing a distorted tetrahedral geometry with a large P−Ag−P angle of 136.71(6)°. The Ag−P (2.4668(18)−2.4753(19) Å) and Ag−O (2.437(5)−2.608(6) Å) bond lengths are normal.[10,14] The two pyrenyl rings are nearly parallel (a dihedral angle = 8°), and are arranged in a rotationally staggered conformation with the angle between the two long axes of pyrenyl rings being 73.7°(Figure 1b). The distance between the mean planes of the two pyrenyl rings is 3.383 Å, suggesting the presence of $\pi-\pi$ interaction between the rings.

The metallacyclophanes are linked by OTf ions to form a polymeric chain-like structure. Two oxygen atoms of each OTf anion are bonded to Ag ions in two neighboring metallacyclophanes, forming an eight-membered $Ag_2O_4S_2$ ring which shows a chairlike conformation (Figure 1c).

Complex **2** (Figure 2, Table 3) is a dinuclear metallacyclophane composed of two Cu(I) ions bridged by two L ligands. In addition to the two P atoms of L, each Cu(I) ion is coordinated to two MeCN molecules, showing a distorted tetrahedral geometry. The Cu−P (2.264(2)−2.311(2) Å) and Cu−N (2.041(6)−2.059(6) Å) bond lengths are normal.[15]

The two pyrenyl rings in **2** are parallel and separated by 3.462 Å. They show a conformation in which the rings are displaced slightly along the long and short axes. There are short contacts between the anions PF_6^- and H atoms from pyrene rings and MeCN (Figure 2a). The C−H···F distances d(C−H···F), ranging from 2.283 Å to 2.642 Å, are shorter than the sum of van der Waals radii (2.67 Å) of H (1.20 Å) and F (1.47 Å), suggesting the presence of weak C−H···F interactions.[16]

Complex **3** displays a dinuclear metallacyclic structure similar to those of **1** and **2** (Figure 3, selected bond lengths and angles are listed in Table 4), composed of two ligands L linked by two Cu(I) ions. The two Cu(I) ions are coordinated to two P atoms and one iodide ion, showing a distorted trigonal planar geometry. The Cu−P (2.268(5)−2.277(6) Å) and Cu−I (2.530(3)−2.536(3) Å) are typical.[17] The two parallel pyrene rings, separated by 3.371 Å, are staggered with a rotated sandwich conformation similar to that of **1**. The angle between the long axes of the two pyrenyl rings is 73.1° (Figure 3b).

Compound **4** is a three-coordinated Ag(I) complex, in which the metal is coordinated to P atoms of two L′ and O atom of an OTf ion (Figure 4, Table 5 for selected bond lengths and angles). The Ag−P (2.4540(12)−2.4618(12) Å) and Ag−O (2.405(3) Å)

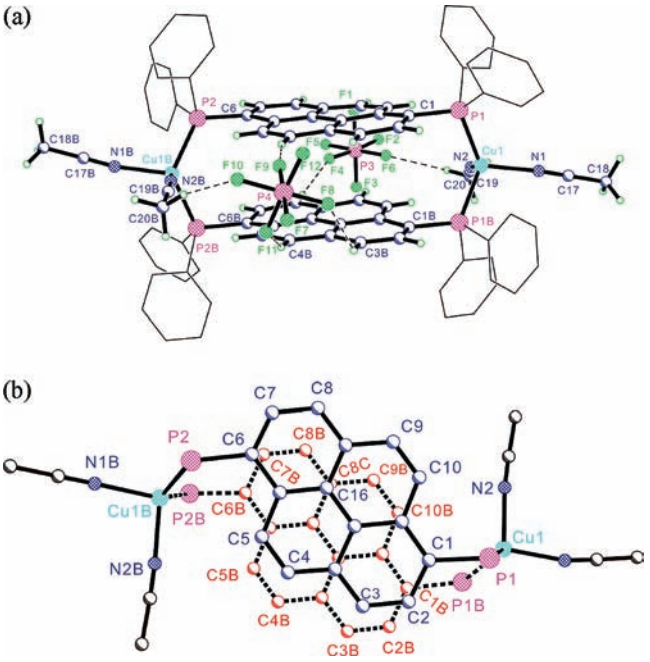

Figure 2. (a) ORTEP diagram of $2 \cdot (PF_6)_2 \cdot CH_3CN \cdot Et_2O \cdot 0.5H_2O$ (50% thermal ellipsoids). Solvent and H atoms are omitted and phenyl rings are shown in wire-frame style for clarity; (b) top view showing the laterally- and axially-displaced sandwich conformation of the pyrene rings.

Table 3. Selected Bond Lengths and Angles for $2 \cdot (PF_6)_2 \cdot CH_3CN \cdot Et_2O \cdot 0.5H_2O$

bond lengths (Å)		bond angles (deg)	
Cu(1)−P(1)	2.264(2)	N(1)−Cu(1)−N(2)	94.7(2)
Cu(1)−N(1)	2.058(6)	N(2)−Cu(1)−P(1)	111.66(17)
Cu(1B)−P(2)	2.3091(18)	N(1)−Cu(1)−P(1)	116.32(16)
Cu(1B)−N(1B)	2.044(6)	N(2)−Cu(1)−P(3)	107.51(16)
		N(1)−Cu(1)−P(3)	105.64(17)
		P(1)−Cu(1)−P(3)	118.20(7)

bond lengths are comparable to those observed in **1**. The complex shows an open dimer structure in which two pyrene rings are not parallel, showing with a dihedral angle of 52.2° and their centers separated by 5.411 Å. However, intermolecular $\pi-\pi$ stacking of pyrene rings is observed in the crystal packing (Figure 4b) where the interacting rings are parallel and separated by 2.961 Å. The two pyrene rings are staggered in a laterally- and axially-displaced conformation.

The molecular structure of **5** (Figure 5 and Table 6) shows two Au(I) ions which are coordinated to a chloride ion and a P atom of L. The Au ions show linear coordination geometry, and the Au−P (2.220(4) −2.228(4) Å) and Au−Cl (2.265(5)−2.281(5) Å) bond lengths are normal.[18] The two Au ions adopt an *anti*-orientation. No $\pi-\pi$ stacking of pyrene rings is found.

The molecular structure of **6** (Figure 6) shows two diphenylphosphine oxide groups (P═O bond length = 1.4854(13) Å) in an *anti*-orientation. No $\pi-\pi$ stacking between pyrenyl or phenyl rings is observed.

NMR Spectroscopy. Similar to the free ligand L, the solution ^1H NMR spectra of the metallacyclophanes show doublets corresponding to the protons of the pyrene rings (Supporting Information,

dx.doi.org/10.1021/ic102441b |*Inorg. Chem.* 2011, 50, 7429–7439

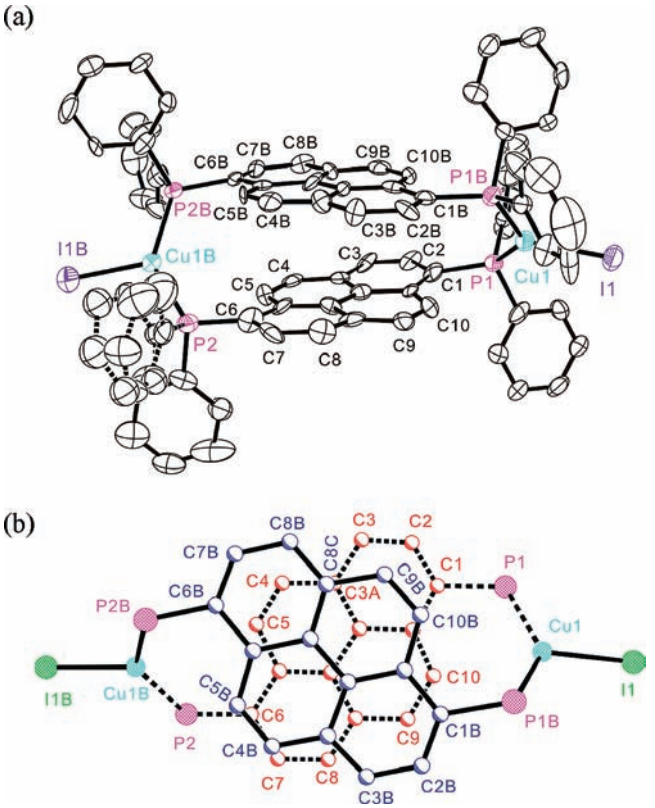

Figure 3. (a) ORTEP diagram of $3 \cdot CH_2Br_2Et_2O$ (50% thermal ellipsoids). One phenyl ring of P(2) is disordered into two positions with 55:45 occupancy. H atoms and solvent molecules are omitted for clarity; (b) top view showing the rotated conformation of the two pyrene rings.

Table 4. Selected Bond Lengths and Angles for $3 \cdot CH_2Br_2 \cdot Et_2O$

bond lengths (Å)		bond angles (deg)	
Cu(1)−P(1)	2.268(5)	P(1)−Cu(1)−P(1B)	129.6(2)
Cu(1)−P(1B)	2.273(5)	P(1)−Cu(1)−I(1)	110.47(15)
Cu(1)−I(1)	2.536(3)	P(1B)−Cu(1)−I(1)	119.18(16)

Figure S2). However, all the pyrene signals of the complexes are significantly upfield shifted from those of L by 0.18 ppm to 1.16 ppm. For instance, the $H_{5,10}$ for **1**, **2**, and **3** are upfield shifted that of L by 0.73, 0.94, and 0.79 ppm, respectively. The shift is attributed to the diatropic shielding experienced by the protons of two stacking pyrene rings. Similar upfield shifts were well documented in some systems having stacking pyrene rings.[19] The upfield shifts of $H_{2,7}$ and $H_{3,8}$ ($\Delta\delta$ = 0.18−0.55 ppm) are smaller than those of $H_{5,10}$ and $H_{4,9}$ ($\Delta\delta$ = 0.73−1.16 ppm). It is consistent with their X-ray crystal structures which show that $H_{2,7}$ and $H_{3,8}$ are generally less covered by the other pyrenyl ring as compared to $H_{5,10}$ and $H_{4,9}$ and hence should be less affected by its anisotropic ring current. It is clear that the metallacyclic structures observed in the crystals of **1**−**3** retain in high concentration solution (10^{-2} M) used in NMR measurements. Interestingly, although the two pyrene rings of **4** are not cofacial in its crystal structure, the signals for pyrene protons are upfield shifted from that of L′. It suggests intramolecular overlap of the pyrene rings in solution. In contrast, the pyrene proton signals observed for the monomeric **5** and **6** are downfield shifted from that of L, probably because

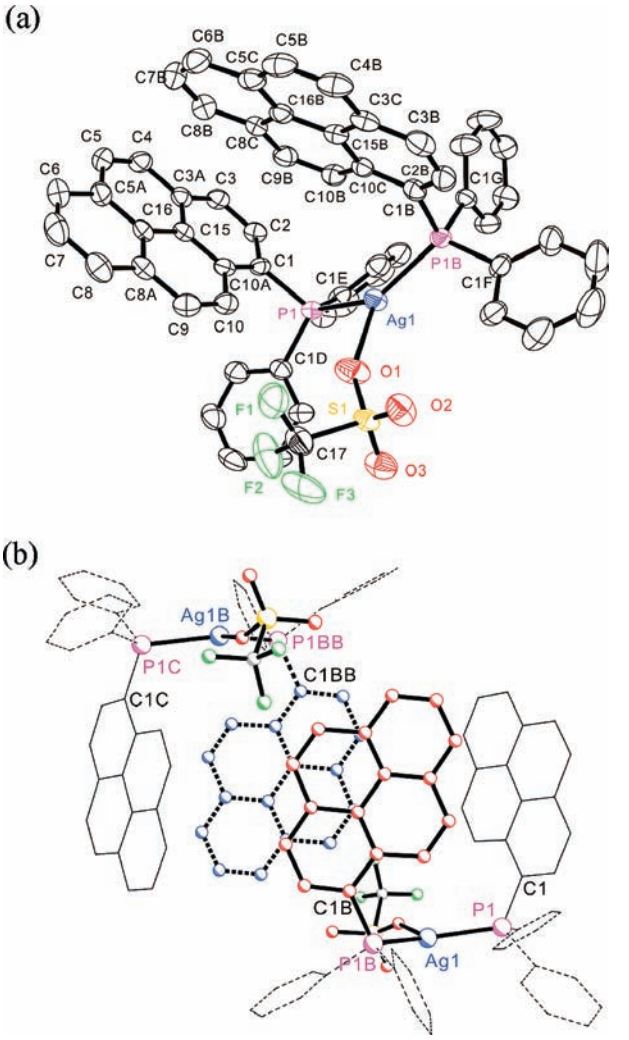

Figure 4. (a) ORTEP diagram of **4** (50% thermal ellipsoids). H atoms are omitted for clarity; (b) top view showing intermolecular $\pi-\pi$ stacking.

Table 5. Selected Bond Lengths and Angles for 4

bond lengths (Å)		bond angles (deg)	
Ag(1)−O(1)	2.405(3)	P(1)−Ag(1)−O(1)	101.92(10)
Ag(1)−P(1B)	2.4540(12)	P(1)−Ag(1)−P(1B)	143.82(4)
Ag(1)−P(1)	2.4618(12)	P(1B)−Ag(1)−O(1)	112.64(10)

of electron-withdrawing effect of the Au(I) ion and phosphine oxide in the compounds.

The $^{31}P\{^1H\}$ NMR spectra of **1**−**3** show only one set of signals. The spectrum of **1** at 300 K shows two characteristic doublets centered at δ 3.98 with $^1J(^{107}Ag-P)$ = 478 Hz and $^1J(^{109}Ag-P)$ = 551 Hz. The spectrum of **2** shows a sharp singlet at δ −4.14 because of the coordinated L. For **3**, a sharp singlet at δ −7.66 ppm is observed. The spectra are essentially unchanged upon cooling from 300 to 193 K, indicating that either there is only one species present in the solution at 300 to 193 K, or even if the complexes dissociate in solution, the dissociation constants are too small for any species arising from the dissociation to be detectable by the spectroscopy (vide infra).

dx.doi.org/10.1021/ic102441b |*Inorg. Chem.* 2011, 50, 7429–7439

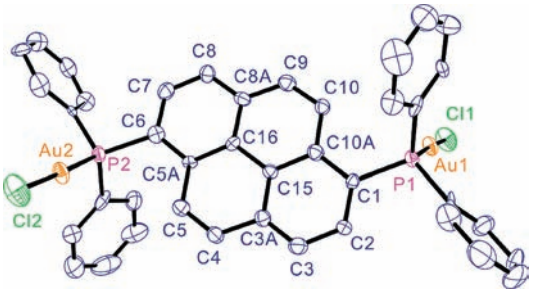

Figure 5. ORTEP diagram of **5** (50% thermal ellipsoids). H atoms are omitted for clarity.

Table 6. Selected Bond Lengths and Angles for 5

bond lengths (Å)		bond angles (deg)	
Au(1)−P(1)	2.228(4)	P(1)−Au(1)−Cl(1)	176.12(18)
Au(1)−Cl(1)	2.281(5)	P(2)−Au(2)−Cl(2)	177.6(2)

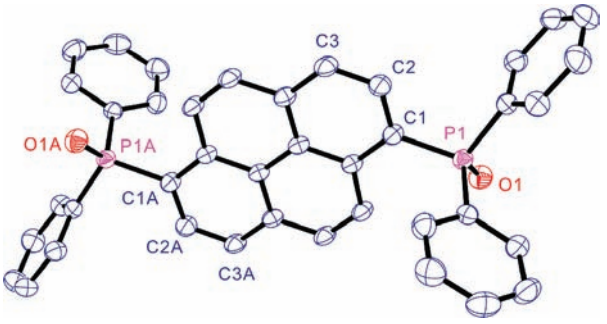

Figure 6. ORTEP diagram of **6** (50% thermal ellipsoids). H atoms are not shown for clarity.

Electronic Absorption Spectroscopy. The UV−vis spectral data of **1**−**6** and the ligands are summarized in Table 7.

The absorption spectra of **1**−**3** and L, and **4**−**6** and L′ are depicted in Figures 7 and 8, respectively. The complexes **1**−**6** show one extremely intense band **A** ($\varepsilon = 5 \times 10^4 - 1.4 \times 10^5$ M^{-1} cm^{-1}) in the UV region at 240−250 nm and three intense bands ($\varepsilon \sim 10^4$ M^{-1} cm^{-1}) **B** (270−290 nm), **C** (320−380), and **D** (390−450 nm) in the visible region. The bands **C** and **D** overlap and only part of the latter is discernible. Bands with similar shapes and energy are displayed by L and L′, suggesting that the absorption bands of the complexes are derived from $\pi \rightarrow \pi^*$ transition of the pyrene ring. Pyrene displays four intense absorption bands arising from electronic transitions from HOMO-1, HOMO to LUMO and LUMO+1.[1a,b,20] In Platt's notation,[21] the bands are labeled ^1B_a, ^1B_b, ^1L_a, and ^1L_b which correspond to the bands **A**, **B**, **C**, and **D**. Perturbations of the metal ions and phosphine substituents are evident from the intensification of the band **D** ($\varepsilon_{max} = 1.80 - 4.65 \times 10^4$ M^{-1} cm^{-1}) as the corresponding ^1L_b band of pyrene is forbidden and very weak ($\varepsilon_{max} = 500$ M^{-1} cm^{-1}).[4b,c] Comparing the spectra of L and **1**−**3** shows that the bands of the latter are broadened, and the bands **C** and **D** are red-shifted by 500−1300 cm^{-1}. In addition, the extinction coefficients of the bands **C** and **D** ($1.4-2.7 \times 10^4$ M^{-1} cm^{-1} per pyrenyl ring) are lower than those of L ($2.8-3.0 \times 10^4$ M^{-1} cm^{-1}). The absorption spectra of **4** and L′ are similar except the band **D** of the former is much more prominent. Unlike the other complexes, **5** and **6** show absorption bands with vibronic peaks. In addition, the bands are only slightly red-shifted (~250 cm^{-1}) from those of L′.

The broadening, small bathochromic shifts and decreases in the absorption intensities of the absorption spectra of the metallacyclophanes indicate the presence of exciton coupling between the two chromophores.[2,22] Similar spectral changes have been observed in many di-(1-pyrenyl) substituted systems[23] and organic cyclophanes containing cofacial pyrene rings.[19,24] The exciton broadening suggests that the dimeric metallacycles

Table 7. UV−vis Absorption Spectral Data for 1−6, L and L′ in CH_2Cl_2

	absorption bands **A**−**D**, λ_{max}/nm (extinction coefficient/10^4 M^{-1} cm^{-1})			
compounds	**A**	**B**	**C**	**D**
1	240 (13.83)	277 (4.64) 294 (4.59)	360 (3.46)^{sh}, 375 (5.16)	395 (4.65)
2	244 (11.90)^{sh}	277 (5.06)^{sh} 292 (4.37)^{sh}	360 (3.37)^{sh}, 377 (5.55)	398 (3.17)
3	250 (12.23)	289 (4.58)^{sh} 306 (3.69)^{sh}	372 (3.17)^{sh}, 387 (3.82)	408 (2.77)^{sh}
4	240 (10.7)	275 (4.82) 285 (6.50)	335 (2.66)^{sh}, 350 (4.83) 357 (4.59), 364 (4.93)	381 (1.80)
5	241 (7.56) 249 (5.88)^{sh}	269 (1.83) 279 (3.39) 290 (6.19)	329 (0.74)^{sh}, 346 (2.20) 358 (3.57), 363 (4.44) 371 (3.72), 376 (3.99)	389 (4.21)
6	241 (5.05) 250 (6.17)	265 (1.59) 274 (3.09) 286 (5.03)	334 (1.75)^{sh}, 342 (2.53) 350 (3.56), 359 (4.39) 367 (3.89), 376 (1.06)^{sh}	385 (2.24)
L	249 (6.55)	282 (2.79) 289 (2.78)	369 (2.83)	387 (3.03)
L′	245 (6.05)	274 (2.57) 282 (2.88)	337 (1.92)^{sh}, 360 (2.58)	*a*

^{sh} Shoulder. ^{a} ^1L_b is not resolved.

dx.doi.org/10.1021/ic102441b |*Inorg. Chem.* 2011, 50, 7429–7439

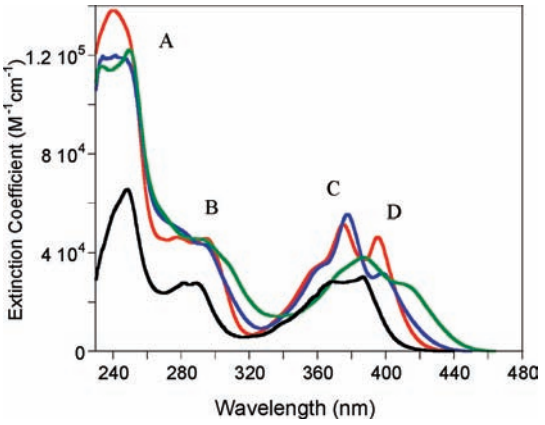

Figure 7. UV−vis spectra of **1** (red), **2** (blue), **3** (green), and L (black) in CH_2Cl_2 at room temperature.

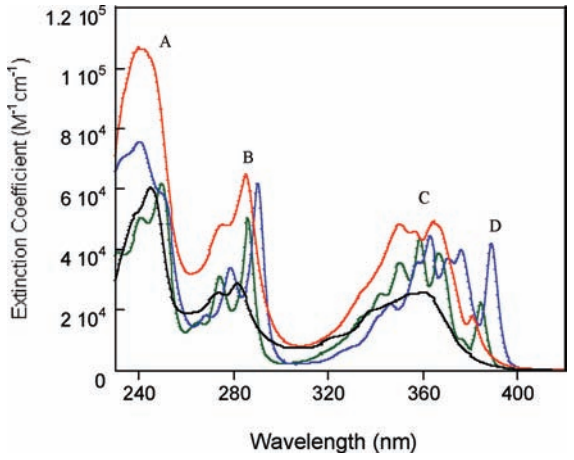

Figure 8. UV−vis spectra of **4** (red), **5** (blue), **6** (green), and L′ (black) in CH_2Cl_2 at room temperature.

are the major species in *freshly prepared* solutions at concentrations as low as 10^{-5} M.

Emission Spectroscopy. Except **3**, all complexes are luminescent. The emission maxima, Stokes shifts, and emission quantum yields are listed in Table 8. The compounds **1**, **2**, and **4** show similar broad unstructured emission bands centered at ∼450−470 nm in solid state and solution. The excitation, solid state and solution emission spectra of **1** are shown in Figure 9. On the other hand, **5** and **6** display emission with vibronic structures centered at ∼380−390 nm (Figure 10).

Complex **1** displays a strong emission with a quantum yield (Φ) of 0.44 in CH_2Cl_2 solution, while the emission of **2** and **4** in CH_2Cl_2 solution are weaker with emission quantum yields of 0.032 and 0.036, respectively. The excitation spectra generally resemble the electronic absorption spectra of the complexes. The Stokes shifts are 3400 cm^{-1}, 3000 cm^{-1}, and 4800 cm^{-1} for **1**, **2**, and **4**, respectively. In addition, the intensity of the emission is not sensitive to the presence of oxygen in the solution, suggesting that the emission is not phosphorescence. In view of the unstructured band shape, the large Stokes shifts, and insensitivity to oxygen, the emissions are attributed to excimeric fluorescence. The energies of the emissions are slightly higher than the excimeric emission of pyrene in solution which peaks at 480 nm.[2]

Table 8. Emission Spectral Data for 1−6[a]

	solution emission λ_{max} (nm) (in CH_2Cl_2)	Stokes shift (cm^{-1})	emission quantum yield Φ (in CH_2Cl_2)	solid state emission λ_{max} (nm)
1	458	3400	0.44	461
2	454	3000	0.032	∼469[b]
3	*c*	*c*	*c*	*c*
4	467	4800	0.036	449
5	393	160	0.086	*d*
6	387	<50	1.00	*d*

[a] All spectra were recorded at room temperature (296 K). [b] It was not able to be determined accurately as the weak emission interfered with the instrument background. [c] No detectable emission. [d] The solid-state emission was not measured.

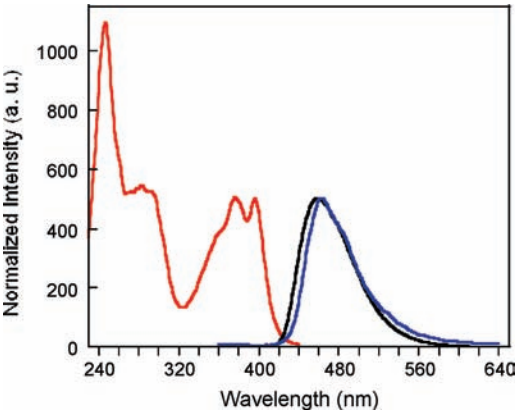

Figure 9. Excitation (red) and emission spectra of **1** (3.20×10^{-4} M) in CH_2Cl_2 (black) and in the solid state (blue) at 297 K.

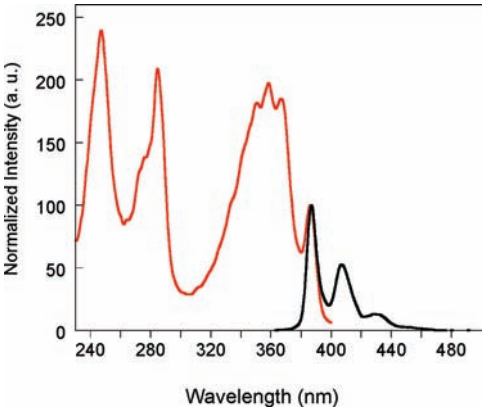

Figure 10. Excitation(red) and emission spectra of **6** in CH_2Cl_2 at 297 K (black).

Complex **3** is not emissive in the freshly prepared CH_2Cl_2 solution and in the solid state at 296 K and at 77 K. The Cu(I) ions are coordinated to electron-donating iodide ions and should be more reducing than the metal centers in **1** and **2** which are coordinated to the poor electron-donating OTf^- ion and MeCN. It is therefore possible that the emission of the pyrenyl ring could be quenched by a rapid intramolecular electron transfer from the Cu(I).

dx.doi.org/10.1021/ic102441b |*Inorg. Chem.* 2011, 50, 7429–7439

Figure 10 depicts the excitation and emission spectra of **6**. The emission (Φ = 0.086) of complex **5** shows a peak at 393 nm which is separated from a vibronic shoulder by ~1250 cm^{-1}. Compound **6** displays similar vibronic emission with much stronger intensity at 387 nm (Φ = 1.0). In view of the small Stokes shift (<50 cm^{-1}), the emissions are assigned to the $S_1 \rightarrow S_0$ fluorescence of the pyrenyl ring.

No monomeric emission, as exemplified by those displayed by **5** and **6**, was observed for the freshly prepared solutions of the complexes **1**, **2**, and **4** even in concentration as low as 10^{-5} M. Moreover, the solution and solid state emissions of the complexes have very similar energies and band shapes. It suggests that the ring structures of the complexes are retained in the solution, as evident from the NMR and UV−vis spectra.

The Stokes shifts between the band **D** and the excimeric emissions of **1** and **2** are 3400 cm^{-1} and 3000 cm^{-1}, respectively, and are smaller than the corresponding shift of the solution excimeric emission of pyrene (~6000 cm^{-1}).[25] The small Stokes shift could be due to the staggered conformation of the pyrene rings as the excimer is most stable when the rings are eclipsed, and any deviations from the conformation would lead to blue shift of the excimeric emission.[2,6a,8c,8d,23e,26] Furthermore, the rigidity of the macrocyclic structures of **1** and **2** would prevent the rings from changing their orientation or shortening their separation. Complex **4** displays an excimeric emission with a larger Stokes shift of 4800 cm^{-1}. The complex with its open dimeric structure should be more flexible than the rigid metallacyclophanes, and hence it should be able to undergo structural changes to reach a favorable excimeric conformation and, as a result, a lower energy excimeric emission.

Dissociation of the Metallacyclophanes. Previous studies of our group and others showed that combining Ag(I) ion and diphosphines led to discrete metallacycles and polymeric helices;[10c] which can undergo exchange dynamics in solution. The propensity could be due to the kinetic liability of the Ag−P bond.[10c,27] The ^1H and $^{31}P\{^1H\}$ NMR, electronic absorption, and emission spectroscopy indicate that the macrocyclic structures of **1**− **3** are retained in the solutions with concentrations as low as 10^{-5} M. The extent of dissociation increases as the concentration of the metallacyclophane decreases.[28] For example, the overall dissociation constant of **1**, K_{dis}, can be expressed as eq 2 where n is number of mole and V is volume of the solution.[28]

$$Ag_2L_2(OTf)_2 \overset{K_{dis}}{\rightleftharpoons} 2AgOTf + 2L \quad (1)$$

$$K_{dis} = \frac{[AgOTf]^2[L]^2}{[\mathbf{1}]} = \frac{n_{AgOTf}^2 \times n_L^2}{n_1 \times V^3} \quad (2)$$

For solutions containing the same *total number* of moles of metallacyclophane and its dissociation products, increase in volume of solvent V (dilution) leads to increase in dissociation products at the expense of the metallacyclophane. To probe the stability of the metallacyclophanes, solution of the complexes in the concentration range of 10^{-7}−10^{-6} M was monitored by absorption and emission spectroscopy.

UV−vis absorption spectra of **1**−**3** in the concentrations range of 1.46×10^{-6}−1.42×10^{-5} M changed very slowly, and distinct changes were only noticed after 1−2 weeks. All spectra showed no isosbestic point, indicating formation of more than one species in the dissociation. Figure 11 shows the spectral changes of *aerated* CH_2Cl_2 solutions of **1** (1.46×10^{-6} M) over nearly 4 months. The spectral changes for **2** and **3** stopped after 3 months, but for **1** the spectral change continued even after 4 months.

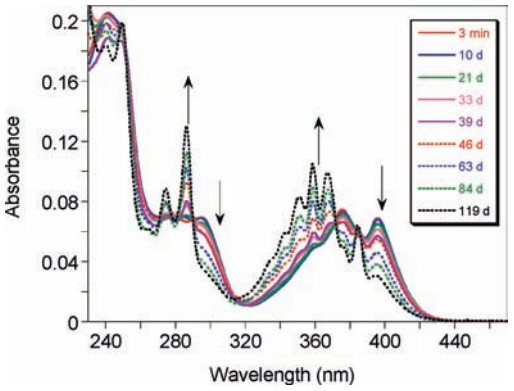

Figure 11. UV−vis absorption spectral change of a solution of **1** in aerated CH_2Cl_2 (conc. = 1.46×10^{-6} M) over 119 days.

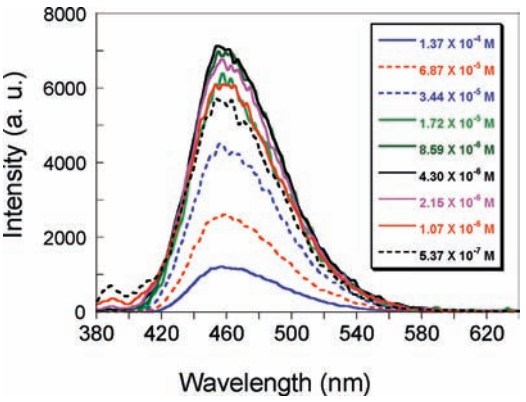

Figure 12. Emission spectra of **1** in CH_2Cl_2 at 1.37×10^{-4}−5.37×10^{-7} M. The emission intensity is normalized to the same concentration. λ_{ex} = 320 nm.

Final spectra of all three complexes resemble the spectrum of the phosphine oxide **6** (Figure 8). Indeed **6** was isolated and confirmed by ^1H NMR and emission spectra. Unlike the aerated solution, degassed CH_2Cl_2 solution of **1** showed very little change over 4 months. Apparently dissolved oxygen is involved in the conversion of **1**−**3** to **6** by oxidizing PPh_2 groups arising from metal-P bond dissociation. Cleavage of the Ag/Cu−P bond led to dangling PPh_2 groups which are prone to air-oxidation.

Emission is a more sensitive spectroscopic handle to follow the decomposition of the metallacycophanes. Emission spectra of **1** (5.50×10^{-4} to 5.37×10^{-7} M) and **2** (1.65×10^{-4} to 2.16×10^{-7} M) at different concentrations were recorded immediately after preparations (Figure 12). For both complexes, the emission maxima did not change with the concentration. However, lowering the concentration increased the quantum yield of the excimeric emission which reached maximum at concentrations ~10^{-6} M (Figure 13). Further dilution (<10^{-6} M) led to a decrease in the quantum yield of the excimeric emission, and new emission peaks appeared at ~380−400 nm. It should be emphasized that the spectra were still dominated by the excimeric emission even at 10^{-7} M, indicating that the metallacyclophanes are intrinsically stable with formation constant ($1/K_{dis}$) ≥ 10^7.

The plots of the emission quantum yields versus concentrations are shown in Figure 13. Both complexes show a linear

dx.doi.org/10.1021/ic102441b |*Inorg. Chem.* 2011, 50, 7429–7439

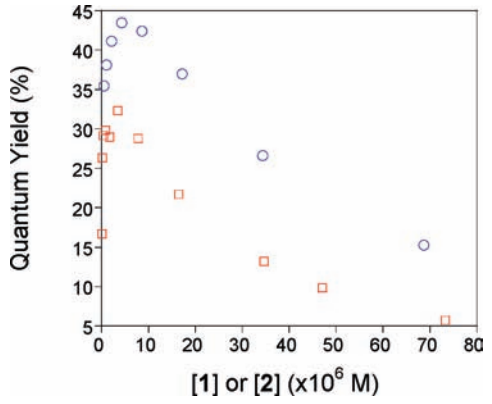

Figure 13. Plots of emission quantum yields versus concentrations for **1** (blue circle) and **2** (red square). The emission quantum yields for **2** have been multiplied by 10.

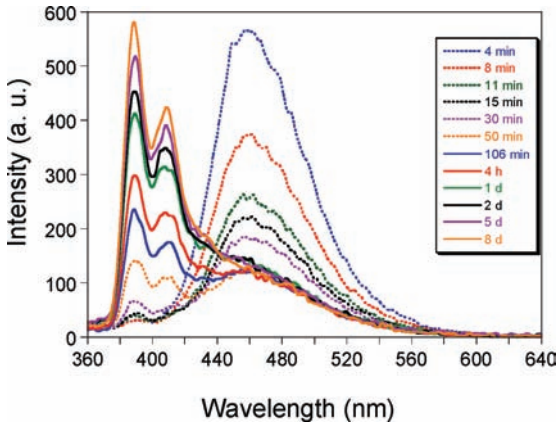

Figure 14. Change in emission of **1** in aerated CH_2Cl_2 (1.34×10^{-6} M) in 8 d.

decrease in emission quantum yield at $\geq 10^{-5}$ M, probably because of self-quenching. On the other hand, there was a sharp decrease in emission quantum yield at $<3-4 \times 10^{-6}$ M. The weak emission around 380−420 nm observed at $<10^{-6}$ M (Figure 12) is probably due to species arising from ring dissociation.

Figure 14 shows the emission change of an aerated 1.34×10^{-6} M CH_2Cl_2 solution of **1** over 8 days. The first emission spectrum, recorded 4 min after the preparation, displayed an intense excimeric emission centered at ~460 nm and a very weak emission at 380−420 nm. The intensity of the excimeric emission decreased rapidly to ~30% of the original within 30 min. Subsequently, the emission intensity centered at ~460 nm was nearly unchanged even after 8 days. The high energy emission increased much slower than the decrease of the excimeric emission, and it continued to rise even after the excimeric emission ceased decreasing.

The vibronic emissions in 380−420 nm are due to the products of decomposition. The final emission spectrum resembles that of **6**. The excitation spectrum with λ_{em} = 412 nm, recorded after 5 days, is essentially the same as the excitation spectrum of **6** (Supporting Information, Figure S4). The fact that the growth of the 380−420 nm emission is much slower than the decrease of the excimeric emission implies that the dissociation of the metallacyclophane gives rise to intermediates which are slowly oxidized by O_2 to **6**, and *the intermediates are probably nonemissive or weakly emissive*. It is reasonable to assume that the intermediates must contain dangling PPh_2 groups as the dissociation must involve cleavage of Ag−P bond. It is possible that the pyrenyl-based emission of the intermediates is quenched by electron transfer from the lone pairs of the PPh_2 groups.[29] In this regard, it should be noted that the free ligand L and L′ are not emissive.

The copper metallacyclophanes **2** and **3** show similar decomposition and ligand oxidation but only faster and more complete. For example, the excimeric emission of **2** (1.03×10^{-6} M) completely vanishes in 1 day (Supporting Information, Figure S5). While a solution of **3** (2.50×10^{-6} M) displays no excimeric emission, an intense vibronic emission in 380−420 nm attributed to the oxidized phosphine is observed in 1 day (Supporting Information, Figure S6). After 7 days, the spectra of **2** and **3** show only the emission of **6**. The reason for the faster decomposition of the copper metallacyles is not clear.

The emission spectrum of a 6.7×10^{-7} M solution of **4** showed complete disappearance of the excimeric emission in 2 days. The final spectrum exhibited a vibronic band in 380−420 nm which resembled the emission of the oxidized ligand 1-(diphenylphosphine-oxide)pyrene (Supporting Information, Figure S7). The fast dissociation and ligand oxidation indicates that the open dimer is less stable than the metallacyclophanes and is therefore more prone to dissociation at low concentration.

CONCLUSION

In this work, the coordination chemistry of two pyrene-bearing phosphines and d^{10} Ag(I) and Cu(I) ions was explored. Our results showed that combining L and the metal ions invariably led to formation of $[Ag_2L_2]^{2+}$ and $[Cu_2L_2]^{2+}$ metallacyclophanes in which two pyrene rings are in staggered cofacial orientation which gives rise to intramolecular excimeric emission which was used as a spectroscopic handle to monitor the stability of the complexes. The metallacyclophanes are stable toward dissociation even at 10^{-7} M, but the dissociation can be driven by air-oxidation of L to phosphine oxide **6**.

ASSOCIATED CONTENT

Supporting Information. ESI mass spectra of compound **3** and NMR spectra of L and complexes **1**−**5**, excitation spectra of **1** and emission spectra of **2**, **3**, and **4** at different times, and X-ray crystallographic data for **1**−**6** in CIF format. This material is available free of charge via the Internet at http://pubs.acs.org.

AUTHOR INFORMATION

Corresponding Author
*E-mail: chmyiphk@nus.edu.sg.

ACKNOWLEDGMENT

We are grateful to Prof. Koh Lip Lin and Ms. Tan Geok Kheng for determining the X-ray structures. The Ministry of Education (R-143-000-429-112), Singapore, and the National University of Singapore are thanked for financial support.

REFERENCES

(1) (a) Birks, J. B. *Photophysics of Aromatic Molecules*; Wiley-Interscience: London, 1970. (b) Kessinger, M.; Michl, J. *Excited States and Photochemistry of Organic Molecules*; Wiley-VCH: New York, 1995.

(c) Turro, N. J. *Modern Molecular Photochemistry*; Benjamin: Menlo Park, NJ, 1978.
(2) Winnik, F. M. *Chem. Rev.* **1993**, *93*, 587.
(3) (a) Mohamed, A. A.; Rawashdeh-Omary, M. A.; Omary, M. A.; Fackler, J. P., Jr. *Dalton Trans.* **2005**, 2597. (b) Burress, C.; Elbjeirami, O.; Omary, M. A.; Gabbaï, F. P. *J. Am. Chem. Soc.* **2005**, *127*, 12166. (c) Che, C.-M.; Chao, H.-Y.; Miskowski, V. M.; Li, Y.; Cheung, K.-K. *J. Am. Chem. Soc.* **2001**, *123*, 4985. (d) Chao, H.-Y.; Lu, W.; Li, Y.; Chan, M. C. W.; Che, C.-M.; Cheung, K.-K.; Zhu, N. *J. Am. Chem. Soc.* **2002**, *124*, 14696. (e) Osawa, M.; Hoshino, M.; Akita, M.; Wada, T. *Inorg. Chem.* **2005**, *44*, 1157.
(4) (a) Partyka, D. V.; Esswein, A. J.; Zeller, M.; Hunter, A. D.; Gray, T. G. *Organometallics* **2007**, *26*, 3279. (b) Heng, W. Y.; Hu, J.; Yip, J. H. K. *Organometallics* **2007**, *26*, 6760. (c) Hu, J.; Yip, J. H. K.; Ma, D.-L.; Wong, K.-Y.; Chung, W.-H. *Organometallics* **2009**, *28*, 51.
(5) For example: (a) Xu, Z.; Singh, N. J.; Lim, J.; Pan, J.; Kim, H. N.; Park, S.; Kim, K. S.; Yoon, J. *J. Am. Chem. Soc.* **2009**, *131*, 15528. (b) Zeng, L.; Wu, J.; Dai, Q.; Liu, W.; Wang, P.; Lee, C. S. *Org. Lett.* **2010**, *12*, 4014. (c) Kim, H. J.; Kim, S. K.; Lee, J. Y.; Kim, J. S. *J. Org. Chem.* **2006**, *71*, 6611. (d) Sakaki, D. Y.; Padilla, B. E. *Chem.Commun.* **1998**, 1581. (e) Nishizawa, S.; Kato, Y.; Teramae, N. *J. Am. Chem. Soc.* **1999**, *121*, 9463. (f) Shiraishi, Y.; Tokitoh, Y.; Hirai, T. *Org. Lett.* **2006**, *8*, 3841. (g) Suzuki, Y.; Morozumi, T.; Nakamura, H.; Shimomura, M.; Hayashita, T.; Bartsch, R. A. *J. Phys. Chem. B* **1998**, *102*, 7910.
(6) (a) De Schryver, F. C.; Collart, P.; Vandendriessche, J.; Goedeweeck, R.; Swinnen, A.; Auweraer, V. d. *Acc. Chem. Res.* **1987**, *20*, 159. (b) Saigusa, H.; Lim, E. C. *Acc. Chem. Res.* **1996**, *29*, 171.
(7) (a) Irngartinger, H.; Kirrstetter, R. G. H.; Kreiger, C.; Rodewald, H.; A., S. H. *Tetrahedron Lett.* **1977**, 1425. (b) Declercq, D.; Delbeke, P.; De Schryver, F. C.; Van Meervelt, L.; Miller, R. D. *J. Am. Chem. Soc.* **1993**, *115*, 5702.
(8) (a) Yang, R.-H.; Chan, W.-H.; Lee, A. W. M.; Xia, P.-F.; Zhang, H.-K.; Li, K. A. *J. Am. Chem. Soc.* **2003**, *125*, 2884. (b) Martínez, R.; Espinosa, A.; Tárraga, A.; Molina, P. *Org. Lett.* **2005**, *7*, 5869. (c) Yang, J.-S.; Lin, C.-S.; Hwang, C.-Y. *Org. Lett.* **2001**, *3*, 889. (d) Kim, S. K.; Bok, J. H.; Bartsch, R. A.; Lee, J. Y.; Kim, J. S. *Org. Lett.* **2005**, *7*, 4839. (e) Inouye, M.; Fujimoto, K.; Furusyo, M.; Nakazumi, H. *J. Am. Chem. Soc.* **1999**, *121*, 1452. (f) Hayashi, H.; Matsumura, N.; Mizuno, K. *J. Chem. Res.* **2004**, 599.
(9) (a) Yam, V. W.-W. *Acc. Chem. Res.* **2002**, *35*, 555. (b) Ghosh, S.; Mukherjee, P. S. *Organometallics* **2008**, *27*, 316. (c) Lin, R.; Yip, J. H. K.; Zhang, K.; Koh, L. L.; Wong, K.-Y.; Ho, K. P. *J. Am. Chem. Soc.* **2004**, *126*, 15852. (d) Thanasekaran, P.; Liao, R.-T.; Liu, Y.-H.; Rajendran, T.; Rajagopal, S.; Lu, K.-L. *Coord. Chem. Rev.* **2005**, *249*, 1085.
(10) (a) James, S. J. *Macromol. Symp.* **2004**, *209*, 119. (b) James, S. L.; Xu, X. L.; Law, R. V. *Macromol. Symp.* **2003**, *196*, 187. (c) Lin, R.; Yip, J. H. K. *Inorg. Chem.* **2006**, *45*, 4423.
(11) Kubas, G. J. *Inorg. Synth.* **1990**, *28*, 68.
(12) Kauffman, G. B. *Inorg. Synth.* **1968**, *11*, 215.
(13) (a) *SMART & SAINT Software Reference Manuals*, Version 4.0; Siemens Energy & Automation, Inc., Analytical Instrumentation: Madison, WI, 1996. (b) Sheldrick, G. M. *SADABS: a Software for Empirical Absorption Corrections*; University of Göttingen: Göttingen, Germany, 2001. (c) *SHELXTL Reference Manual*, Version 5.03; Siemens Energy & Automation, Inc., Analytical Instrumentation: Madison, WI, 1996.
(14) Brandys, M.-C.; Puddephatt, R. J. *J. Am. Chem. Soc.* **2002**, *124*, 3946.
(15) (a) Hanna, J. V.; Boyd, S. E.; Healy, P. C.; Bowmaker, G. A.; Skelton, B. W.; White, A. H. *Dalton Trans.* **2005**, *15*, 2547. (b) Barron, P. F.; Dyason, J. C.; Healy, P. C.; Engelhardt, L. M.; Pakawatchai, C.; Patrick, V. A.; White, A. H. *Dalton Trans.* **1987**, 1099.
(16) Bondi, A. *J. Phys. Chem.* **1964**, *68*, 441.
(17) Bowmaker, G. A.; Dyason, J. C.; Healy, P. C.; Engelhardt, L. M.; Pakawatchai, C.; White, A. H. *Dalton Trans.* **1987**, 1089.
(18) Müller, T. E.; Green, J. C.; Mingos, D. M. P.; McPartlin, C. M.; Whittingham, C.; Williams, D. J.; Woodroffe, T. M. *J. Organomet. Chem.* **1998**, *551*, 313.
(19) (a) Umemoto, T.; Satani, S.; Sakata, Y.; Misumi, S. *Tetrahedron Lett.* **1975**, *36*, 3159. (b) Kawashima, T.; Otsubo, T.; Sakata, Y.; Misumi, S. *Tetrahedron Lett.* **1978**, *51*, 5115.
(20) (a) Clar, E. *Spectrochim. Acta* **1950**, *4*, 116. (b) Yoshinaga, T.; Hiratsuka, H.; Tanzaki, Y. *Bull. Chem. Soc. Jpn.* **1977**, *50*, 3096.
(21) Platt, J. R. *J. Chem. Phys.* **1949**, *17*, 484.
(22) (a) Kim, D.; Osuka, A. *Acc. Chem. Res.* **2004**, *37*, 735. (b) Seo, Y. J.; Rhee, H.; Joo, T.; Kim, B. H. *J. Am. Chem. Soc.* **2007**, *129*, 5244.
(23) (a) Yorozu, T.; Hoshino, M.; Imamura, M. *J. Phys. Chem.* **1982**, *86*, 4426. (b) Herkstroeter, W. G.; Martic, P. A.; Farid, S. *J. Chem. Soc., Perkin Trans. 2* **1984**, 1453. (c) Ueno, A.; Suzuki, I.; Osa, T. *J. Am. Chem. Soc.* **1989**, *111*, 6391. (d) Winnik, M. A.; Bystryak, S. M.; Liu, Z.; Siddiqui, J. *Macromolecules* **1998**, *31*, 6855. (e) Nandy, R.; Subramoni, M.; Varghese, B.; Sankararaman, S. *J. Org. Chem.* **2007**, *72*, 938.
(24) Hayashi, T.; Mataga, N.; Umemoto, T.; Sakata, Y.; Misumi, S. *J. Phys. Chem.* **1977**, *81*, 424.
(25) Rohatgi-Mukherjee, K. K. In *Fundamentals of Photochemistry*, revised ed.; Wiley Eastern: New Delhi, 1986.
(26) Tsujii, Y.; Itoh, T.; Fukuda, T.; Miyamoto, T.; Ito, S.; Yamamoto, M. *Langmuir* **1992**, *8*, 936.
(27) (a) Muetterties, E. L.; Alegranti, C. W. *J. Am. Chem. Soc.* **1970**, *92*, 4114. (b) Muetterties, E. L.; Alegranti, C. W. *J. Am. Chem. Soc.* **1972**, *94*, 6386. (c) Lozano, E.; Nieuwenhuyzen, M.; James, S. L. *Chem.—Eur. J.* **2001**, *7*, 2644. (d) Dean, P. A. W; Vittal, J. J.; Srivastava, R. S. *Can. J. Chem.* **1987**, *65*, 2628.
(28) Anslyn, E. V.; Dougherty, D. A. In *Modern Physical Organic Chemistry*; University Science Books: Sausalito, CA, 2006; p 212.
(29) (a) Yamaguchi, S.; Akiyama, S.; Tamao, K. *J. Organomet. Chem.* **2002**, *646*, 277. (b) Smith, R. C.; Protasiewicz, J. D. *Dalton Trans.* **2000**, 4738. (c) Smith, R. C.; Earl, M. J.; Protasiewicz, J. D. *Inorg. Chim. Acta* **2004**, *357*, 4139. (d) Hay, C.; Hissler, M.; Fischmeister, C.; Rault-Berthelot, J.; Toupet, L.; Nyulaszi, L.; Réau, R. *Chem.—Eur. J.* **2001**, *7*, 4222.